

## Electronic Supplementary Information

# Changes of Major Charge Transport by Molecular Spatial Orientation on Graphene Channel Field Effect Transistors

## Experimental Methods

### Materials

*Synthesis of benzene diazonium salts.* Functionalized benzene molecules (e.g., nitrobenzene (phenyl-NO<sub>2</sub>), carboxylbenzene (phenyl-COOH), bromobenzene (phenyl-Br), and aminobenzene (phenyl-NH<sub>2</sub>) and their diazonium *p*-toluenesulfonate salts (e.g., 4-nitrobenzene (N<sub>2</sub><sup>+</sup>-phenyl-NO<sub>2</sub>), 4-carboxylbenzene (N<sub>2</sub><sup>+</sup>-phenyl-COOH), 4-bromobenzene (N<sub>2</sub><sup>+</sup>-phenyl-Br), and 4-aminobenzene (N<sub>2</sub><sup>+</sup>-phenyl-NH<sub>2</sub>) and a benzene diazonium *p*-toluenesulfonate salt (N<sub>2</sub><sup>+</sup>-phenyl-H) were prepared for physisorption and chemisorption, respectively. Benzene diazonium salts were synthesized by using ion exchange resin (e.g., resin-NO<sub>2</sub><sup>-</sup>) with *p*-substituted aniline compounds as described in the previous report.<sup>1</sup>

Sodium nitrite (4.1 g, Aldrich) was added to a solution of ion exchange resin AV-17-8 (7.0 g, Aldrich) in the de-ionized (DI) H<sub>2</sub>O (16 ml) and stirred at room temperature for 20 min. The resulting solid (i.e., resin-NO<sub>2</sub><sup>-</sup>) was filtered, washed with H<sub>2</sub>O until the pH of the filtrate became neutral (pH 6–7), and dried at room temperature for 30 min (a yield of 6.4 g). The resin-NO<sub>2</sub><sup>-</sup> (4.5 g containing 16 mmol NO<sub>2</sub><sup>-</sup>) was added to a solution of monohydrate *p*-toluenesulfonic acid (2.3 g, 16 mmol) in AcOH (8 mL) and stirred for 5 min. The *p*-substituted aniline compound (e.g., 4-bromoaniline, 4-nitroaniline, 4-carboxylaniline, 4-aminoaniline, and aniline) (5.3 mmol) was added to the above solution four times and the mixture was stirred for 5–20 min until TLC indicated complete consumption of the aniline (hexane-ether 1:1). The mixture was filtered from the resin and the filtrate was poured into ether (100–140 mL). The resulting solid was filtered, washed with ether (20–40 mL), and dried under vacuum.

*Graphene oxide and graphene* GO was prepared according to literature procedures, which was characterized by Raman spectroscopy, X-ray diffraction (XRD), and XPS.<sup>2</sup> Large-single layer graphene on Cu foil was supplied from Graphene Center at Sungkyunkwan University, which was characterized by Raman spectroscopy and AFM.<sup>3</sup>

## **Fabrication of molecular functionalized FET devices with different graphenes**

FET devices were composed of channels (5-10  $\mu\text{m}$  length and 25-250  $\mu\text{m}$  width) and the pre-patterned Au source and drain electrodes (50-60 nm thickness) on the  $\text{SiO}_2$  (300 nm thickness)/Si substrate, which were sonicated in DI water, acetone, and EtOH for 10 min, immersed in a piranha solution for 5 min, washed with DI water several times, and dried with  $\text{N}_2$ .

(1) n-RGO channel FETs: Water-dispersed GO solution ( $0.5 \text{ mg mL}^{-1}$ ) was spin-coated on the cleaned FET devices. The GO-coated FET devices were dried at  $80 \text{ }^\circ\text{C}$  in a vacuum oven for 24 h, which can improve the adhesion of GO sheets on the  $\text{SiO}_2/\text{Si}$  substrate. The GO channel FET devices were chemically reduced with a 98% hydrazine ( $\text{N}_2\text{H}_4$ ) hydrate vapor at  $80 \text{ }^\circ\text{C}$  for 24 h. The resulting reduced GO (RGO) channel FET devices were washed with DI water for 1 h and then dried at  $80 \text{ }^\circ\text{C}$  in a vacuum oven for 24 h. Finally, the RGO FET devices were thermally annealed using a process of rapid thermal annealing at  $200\sim 250 \text{ }^\circ\text{C}$ . Thermally annealed  $\text{N}_2\text{H}_4$ -RGO FET devices using rapid thermal annealing produced a nitrogen-doped RGO channels (n-RGO).

(2) p-CVD-G channel FETs: Single layer CVD-G on Cu foil was transferred on the cleaned FET devices using (poly(methyl methacrylate), PMMA)-mediated method as described in the previous paper.<sup>3</sup> Finally, the CVD-G FET devices were thermally annealed using a process of rapid thermal annealing at  $200\sim 250 \text{ }^\circ\text{C}$ . Usually, the CVD-G FET devices showed p-type behaviors (p-CVD-G).

(3) Molecular functionalization of the graphene FETs: the graphene FET devices were immersed in a 70 mM anhydrous DMF solution of the functionalized benzene molecules and the functionalized benzene diazonium tosylate ( $\text{N}_2^+\text{TsO}^-$ ) compounds for physisorption and chemisorption, respectively, in a glove box for 24 h. The functionalized graphene FET devices were thoroughly washed with DMF several times and then dried for  $>24 \text{ h}$  in vacuum desiccators.

## **Measurement of electrical properties**

The source-drain current *versus* the back gate voltage for the FET devices was measured by a 4200 Keithely semiconductor characterization system at room temperature in a vacuum of  $1 \times 10^{-4} - 1 \times 10^{-5}$  torr. Raman spectroscopy (Reinshaw, RM 1000-In Via), XPS (VG microtech ESCA 2000), AFM (SPA 3800, Seiko), TEM (JEOL JEM-2100F) were used for surface characterization. Raman spectroscopy (with 514 nm) was performed under ambient condition.

## Supporting Figures

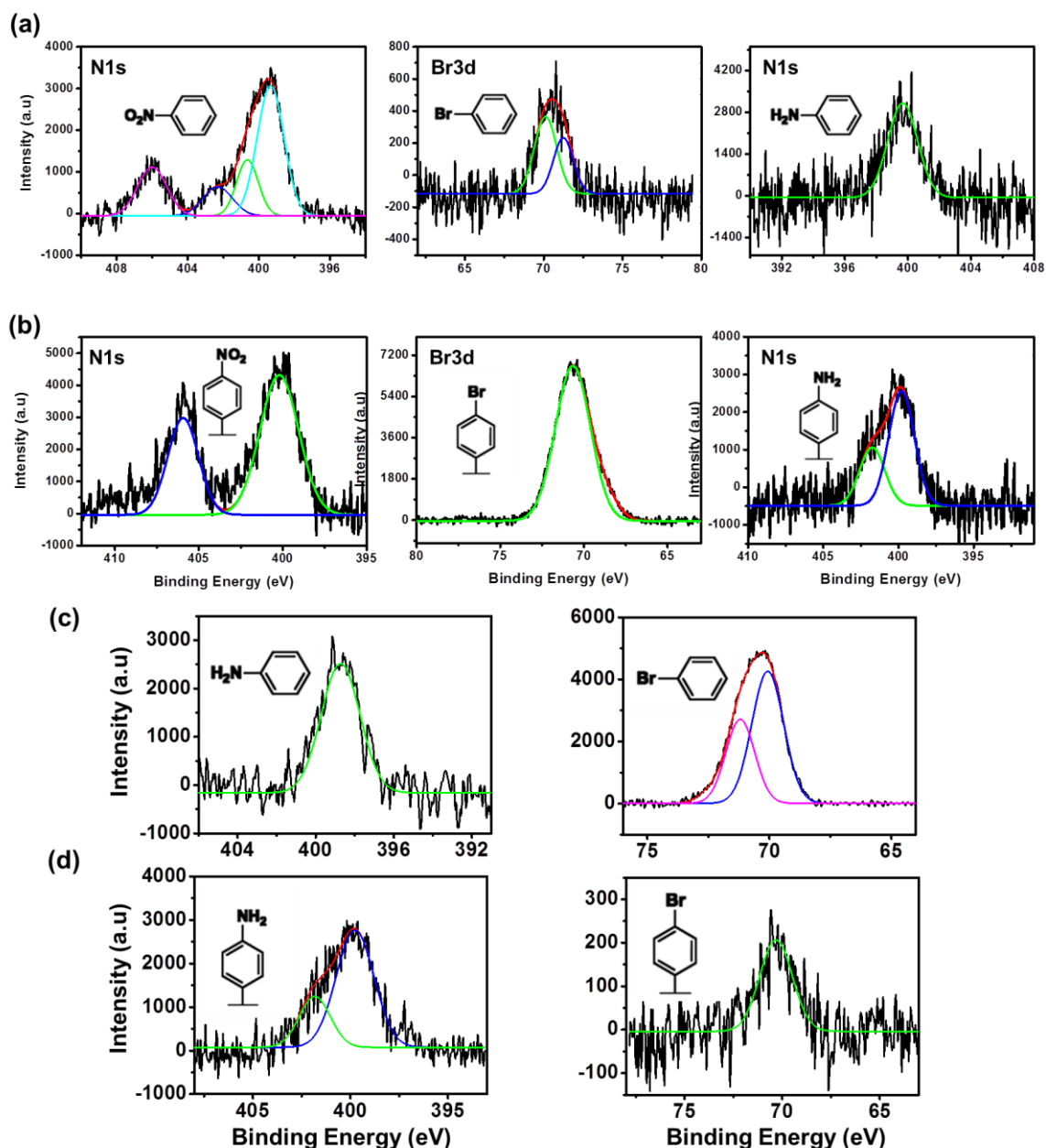


**Fig. S1.** (a) (b) XPS spectra of the functionalized n-RGO channels on FET devices with (a) benzene molecules (e.g., phenyl-NO<sub>2</sub>, phenyl-Br, and phenyl-NH<sub>2</sub>) and (b) benzene diazonium compounds (e.g., N<sub>2</sub><sup>+</sup>-phenyl-NO<sub>2</sub>, N<sub>2</sub><sup>+</sup>-phenyl-Br, and N<sub>2</sub><sup>+</sup>-phenyl-NH<sub>2</sub>). (c) (d) XPS spectra of the functionalized p-CVD-G channels on FET devices with (c) benzene molecules (e.g., phenyl-NH<sub>2</sub> and phenyl-Br) and (b) benzene diazonium compounds (e.g., N<sub>2</sub><sup>+</sup>-phenyl-NH<sub>2</sub> and N<sub>2</sub><sup>+</sup>-phenyl-Br).

High resolution X-ray photoelectron spectroscopy (XPS) could characterize physisorption of the benzene molecules on the n-RGO channels of FET devices (Fig. S1a) and chemisorption of the

benzene diazonium compounds on the n-RGO channels of FET devices (Fig. S1b). The XPS spectra confirmed the existence of N (for  $-\text{NO}_2$  and  $-\text{NH}_2$  groups) and Br (for  $-\text{Br}$  groups) elements on n-RGO for both cases of physisorption and chemisorption. For the physisorption (Fig. S1a), N1s of nitrobenzene was detected at 406.1 eV for  $-\text{NO}_2$  groups (accompanying with an additional peak at 399.5 eV from  $-\text{NH}_2$  groups due to X-ray beam-induced reduction). Br3d of bromobenzene was detected at 70.5 eV. N1s of aminobenzene was detected at 399.6 eV. For the chemisorption (Fig. S1b), N1s of 4-nitrobenzene was detected at 406.0 eV for  $-\text{NO}_2$  groups. Br3d of 4-bromobenzene and N1s of 4-aminobenzene were detected at 70.7 eV and 399.8 eV, respectively. These XPS spectra suggested that the molecular functionalization on the n-RGO channel was successfully prepared. Also, XPS spectra for physisorption and chemisorption of molecules on p-CVD-G (Fig. S1c,d) confirmed the existence of N (for  $-\text{NH}_2$  groups) and Br (for  $-\text{Br}$  groups) elements.

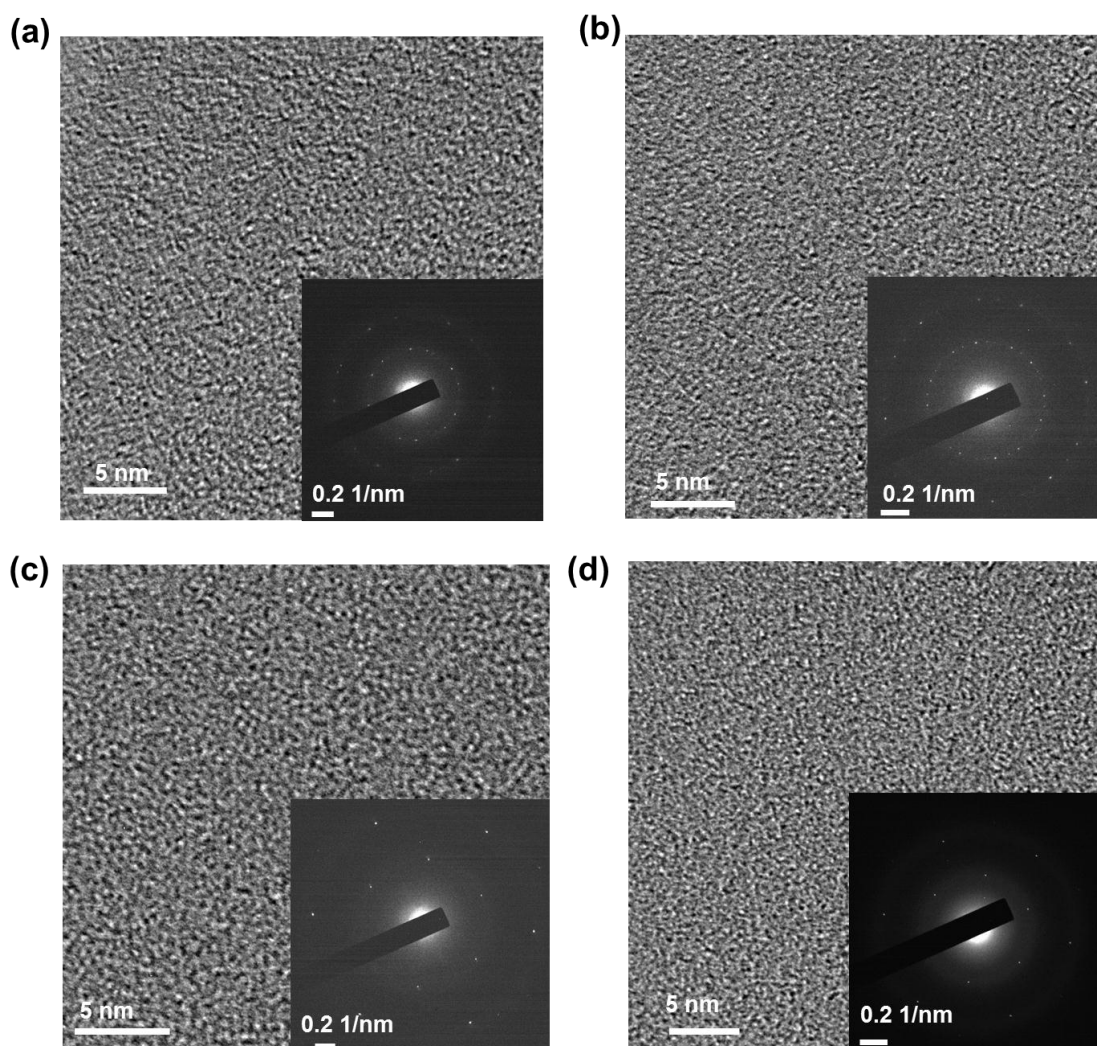
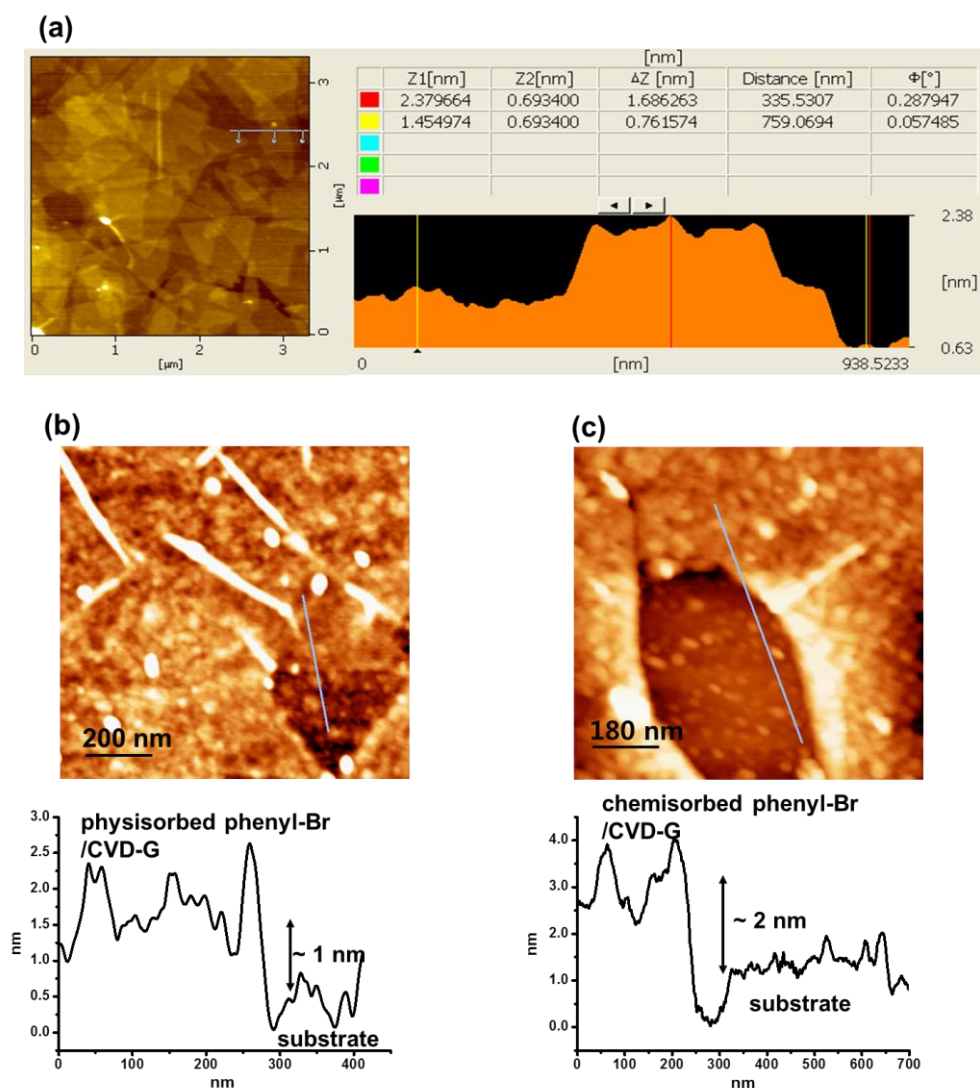


**Fig. S2.** (a) (b) High-resolution transmission electron microscopy (TEM) images and selected area electron diffraction (SAED) patterns of n-RGO after molecular (a) physisorption and (b) chemisorption.

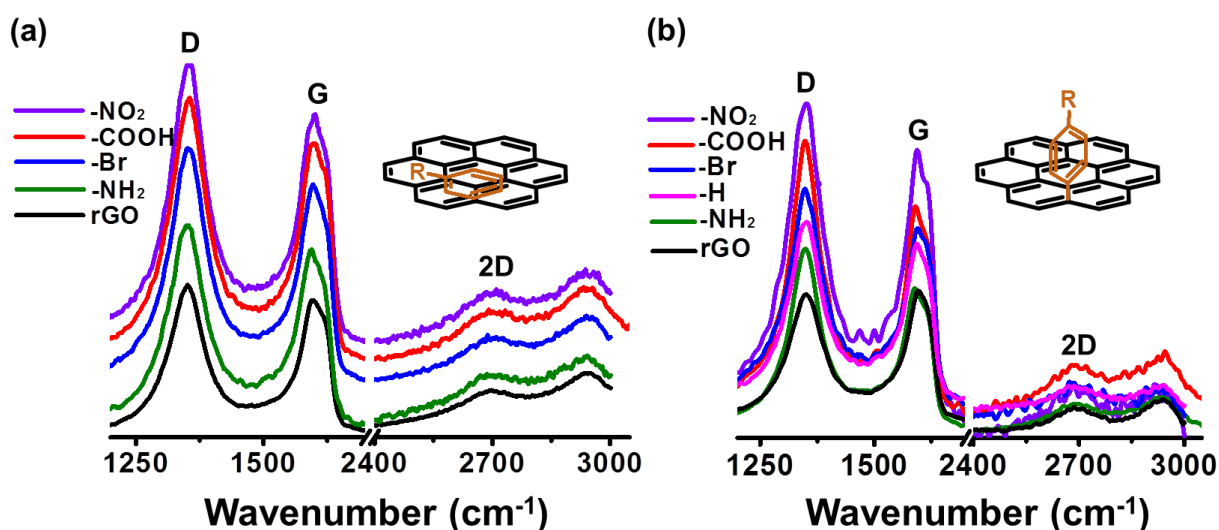


(c) (d) High-resolution TEM images and SAED patterns of p-CVD-G after molecular (c) physisorption and (d) chemisorption.

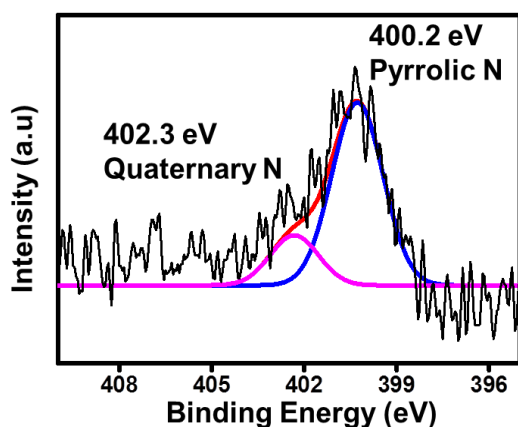
In Fig. S2a and b, the n-RGO channels were fabricated with n-RGO sheets (having a 2~3 micrometers-lateral size) over layered at the each edge of them. The SAED patterns of n-RGO displayed a hexagonally symmetric pattern indicating a bilayer region of n-RGO. Fig. S2a show that the lattice constant was measured with  $2.44\pm 0.01$  Å, similar to that of the intrinsic graphene,<sup>4</sup> indicating that physical functionalization of molecules does not change the conjugated framework of n-RGO. In Fig. S2b, the lattice constant of n-RGO was slightly increased ( $2.48\pm 0.01$  Å) after the chemical functionalization, revealing the expansion of bonding length from C=C  $sp^2$  to C-C  $sp^3$ .<sup>4</sup> In Fig. S2c and d, the SAED patterns displayed a hexagonally symmetric pattern of single-layer graphene, which confirmed that the lattice constant of p-CVD-G also was slightly increased ( $2.49\pm 0.01$  Å) after the chemical functionalization as compared with that ( $2.45\pm 0.02$  Å) of the physical functionalization.



**Fig. S3.** (a) AFM image and line profiles of an n-RGO channel on a FET device. Single or double sheets of n-RGO showed a thickness of 0.76 nm or 1.7 nm from the substrate, respectively. (b) (c) AFM images and line profiles of (b) physisorbed phenyl-Br on p-CVD-G and (c) chemisorbed phenyl-Br on p-CVD-G. Considering the molecular length of phenyl-Br (~0.63 nm calculated with ChemBio3D), thickness of graphene (0.5~0.8 nm in an AFM image), and surface roughness (~0.5 nm), the height (or thickness) difference (~1 nm) between (c) and (d) images imply that chemically functionalized phenyl-Br molecules are vertically attached on the p-CVD-G surface.



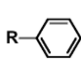
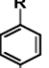
**Fig. S4.** (a) (b) Raman spectra of (a) physically- and (b) chemically-functionalized p-CVD-G frameworks.



**Fig. S5.** XPS spectrum of N 1s for n-RGO.

**Table S1.** Raman peak positions and the  $I(D)/I(G)$  ratios for the D- and the G-bands of the molecularly-

functionalized n-RGO FET devices for Fig. 1a and b.

	D /cm <sup>-1</sup>	G /cm <sup>-1</sup>	I(D)/I(G)		D /cm <sup>-1</sup>	G /cm <sup>-1</sup>	I(D)/I(G)
<b>Pristine</b>	1350	1593	1.12	<b>Pristine</b>	1346	1595	0.9
<b>R = NO<sub>2</sub></b>	1350	1597	1.13	<b>R = NO<sub>2</sub></b>	1350	1593	1.17
<b>COOH</b>	1354	1594	1.14	<b>COO</b>	1343	1591	1.32
<b>Br</b>	1350	1594	1.13	<b>Br</b>	1347	1593	1.21
<b>NH<sub>2</sub></b>	1350	1592	1.08	<b>NH<sub>2</sub></b>	1350	1591	1.27
				<b>H</b>	1351	1593	1.14

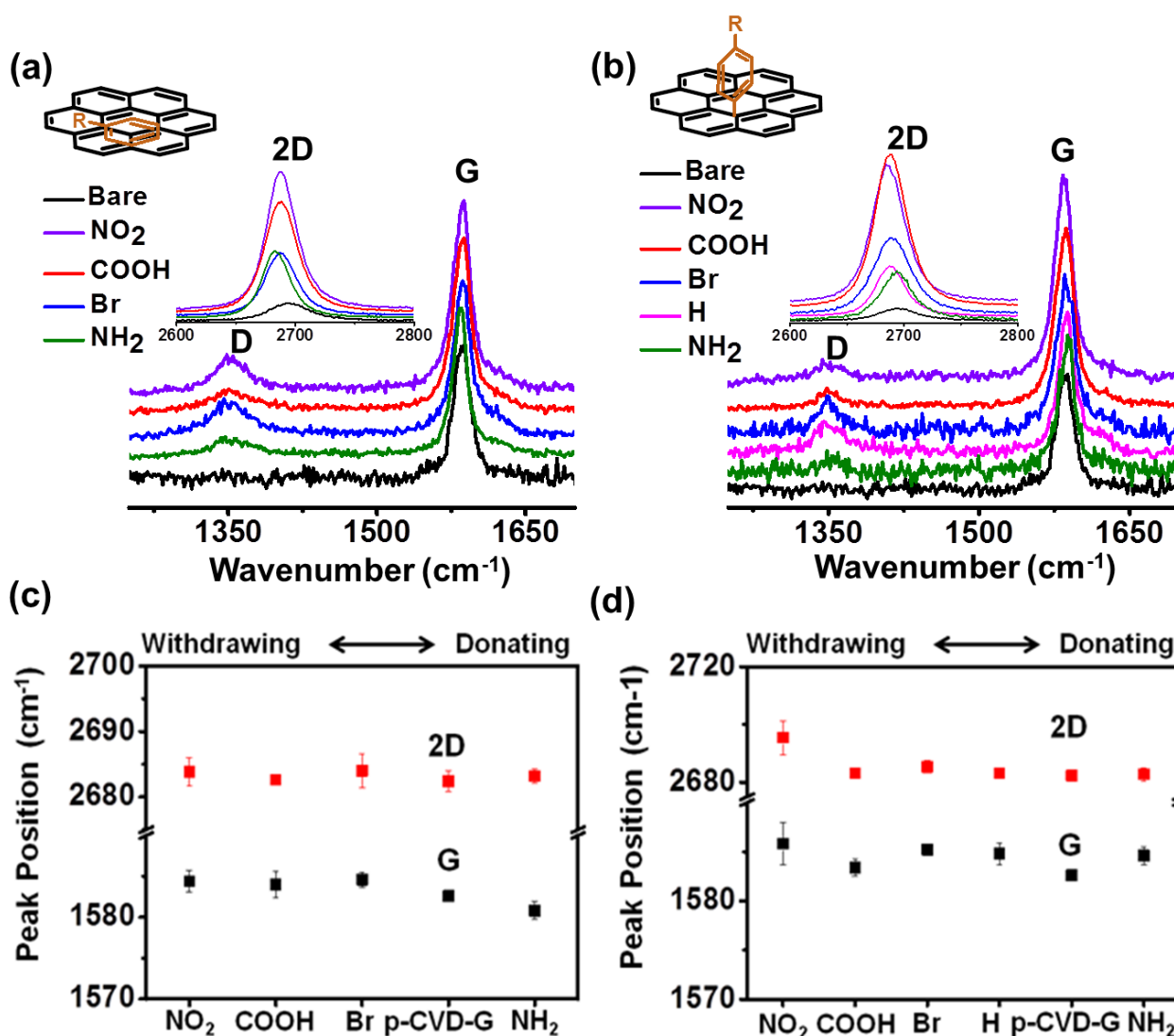


**Fig. S6** (a) (b) Raman spectra of (a) physically- and (b) chemically-functionalized p-CVD-G frameworks. (c) (d) Plots of the peak positions for the G-band and the 2D-band with regard to (c) physically- and (d) chemically-functionalized p-CVD-G frameworks. Peak position plots were average values with the error bars denoting the standard deviations, which were obtained by each 5~10 place with 2~3 samples.

In Raman spectroscopy analysis for molecular functionalized p-CVD-G FETs, the physically adsorbed benzene molecules with the electron withdrawing groups induced a slight up-shift compared to the G-band of the pristine p-CVD-G, while the benzene molecule with the electron donating group induced a down-shift (Fig. S6a). On the other hand, the G-bands of all samples modified with the covalently-bound benzene molecules with different functional groups up-shifted from that of pristine p-CVD-G, indicating that all p-CVD-G channels modified with the covalently-bound benzene molecules produced the only hole-doped p-CVD-G channel (*i.e.*, p-type) (Fig. S6b). Such phenomenon is assumed to come from the p-prone nature of p-CVD-G as reported in the previous literature.<sup>5</sup> Furthermore, the 2D-band for all p-CVD-G samples exhibited the up-shift regardless of the adsorption process or the molecular functionality. The 2D- and G-band shifts revealed molecular doping characteristics for the physical functionalization; n-doping has the 2D- and G-bands shift to the reverse direction while p-doping has those bands shift to the same direction (Fig. S6c).<sup>6</sup> However, molecular doping characteristics for the chemical functionalization of p-CVD-G were not observed; both molecular electron donating or electron withdrawing groups have the 2D- and G-bands shift to the same direction (Fig. S6d). As shown in Fig. 1 for the chemisorption of n-RGO, no effects of functional groups on p-CVD-G covalently bound molecules is assumed by the molecular orientation of new C-C bonds.

### Supporting reference

1. V. D. Filimonov, M. Trusova, P. Postnikov, E. A. Krasnokutskaya, Y. M. Lee, H. Y. Hwang, H. Kim and K.-W. Chi, *Org. Lett.*, 2008, **10**, 3961-3964.
2. I. K. Moon, J. Lee, R. S. Ruoff and H. Lee, *Nat. Commun.*, 2010, **1**, 73.
3. M. S. Choi, S. H. Lee and W. J. Yoo, *J. Appl. Phys.*, 2011, **110**, 073305-073306.
4. H. Zhu, P. Huang, L. Jing, T. Zuo, Y. Zhao and X. Gao, *J. Mater. Chem.*, 2012, **22**, 2063-2068.
5. X. Wang, X. Li, L. Zhang, Y. Yoon, P. K. Weber, H. Wang, J. Guo and H. Dai, *Science*, 2009, **324**, 768-771.
6. X. Dong, D. Fu, W. Fang, Y. Shi, P. Chen and L.-J. Li, *Small*, 2009, **5**, 1422-1426.